Two-dimensional magnetotelluric analysis of three-dimensional bodies: a case study from South Australia

Katherine Broxholme
CRC LEME
Geology and Geophysics
University of Adelaide
Adelaide SA 5005
Katherine.Broxholme@adelaide.edu.au

Graham Heinson
CRC LEME
Geology and Geophysics
University of Adelaide
Adelaide SA 5005
Graham.Heinson@adelaide.edu.au

Stephen Busuttil
MIM Exploration
13 Maple Street
Forrestville
Adelaide SA 5035
sxbusutt@mim.com.au

Ted Lilley
RSES
ANU
GPO Box 4
Canberra ACT 0200
Ted.Lilley@anu.edu.au

SUMMARY

Magnetotelluric (MT) tensors have significantly different forms depending on whether the subsurface is one-dimensional (1D), two-dimensional (2D) or three-dimensional (3D). In subsurface geological structures that are not 1D, two-dimensionality is often assumed, as inversion routines for 2D earth models are computationally more tractable than those for full 3D media. In 2D, the MT tensor decouples into two independent modes, the transverse electric (TE) mode and the transverse magnetic (TM) mode. Often only one of these modes is acquired during commercial operations.

Field data were collected over an elongate magnetic anomaly of a type that would normally be approximated as 2D but which has a finite strike length and is therefore a 3D body. With this in mind, the applicability of interpreting data defined as TE and TM were assessed using (a) Mohr circles galvanic distortion analyses, (b) determination of strike of local and regional geology, and (c) comparison of 2D inversion techniques. The data were collected with the Mount Isa Mines Distributed Acquisition System (MIMDAS) in the Deep Well prospect of the Curnamona Province in South Australia. We show that the TM mode accurately delineates boundaries and that since boundary-charges are included in the inversion formulation, it also provides accurate values of apparent resistivity. The TE mode provides poor boundary delineation and underestimates the resistivity of the 3D body. Joint inversions provide only a small improvement upon TM-only inversions, but determination of dimensionality, strike and detection of galvanic distortion mean that collection of both data modes is still preferable.

Keywords: Magnetotellurics, galvanic distortion, dimensionality, inversion

INTRODUCTION

Magnetotelluric (MT) tensors and the processes used to analyse them are significantly different depending on the dimensionality of the subsurface. All naturally occurring bodies are on some scale 3-dimensional (3D), but current 3D processing and modelling procedures are computationally expensive, so commercially it is generally assumed that anomalies of interest are 2-dimensional (2D). MT fields decouple into two independent modes when they interact with a perfectly 2D subsurface. Defining the x-direction as along strike, the y-direction as perpendicular to strike and the z-direction as vertical and positive downwards, as shown in Figure 1, the xy mode is the transverse electric (TE) mode; and the yx mode is the transverse magnetic (TM) mode. Structures that tend towards this two-dimensionality include faults, folds or shear zones that are approximately linear in the scale of the survey.

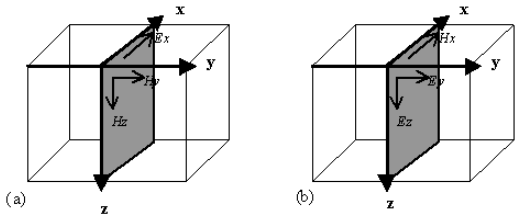

Figure 1. For a 2D structure, the MT response decomposes into two independent modes: (a), the TE mode is dependent on Ex, Hy and Hz; and (b) the TM mode is dependent on Hx, Ey and Ez (after Swift, 1971).

Patra and Mallick (1980) show that the diffusion equation applies to 2D conductivity structures such that

$$\frac{\partial^2 \mathrm{K}}{\partial \mathrm{y}^2} + \frac{\partial^2 \mathrm{K}}{\partial \mathrm{z}^2} = \lambda^2 \mathrm{K} \qquad (1)$$

where $\lambda^2 = i\omega\mu\sigma(y,z)$ and a time dependence of $e^{i\omega t}$ is assumed. For the TM mode, K is replaced by B_x and the electric field components are related to B_x by

$$\frac{\partial B_x}{\partial y} = -\mu\sigma(y,z)E_z \text{ and } \frac{\partial B_x}{\partial z} = \mu\sigma(y,z)E_y \qquad (2)$$

For the TE mode K is replaced by E_x such that the magnetic field components are related to E_x by

$$\frac{\partial E_x}{\partial y} = i\omega B_z \text{ and } \frac{\partial E_x}{\partial z} = -i\omega B_y \qquad (3)$$

Note that the TE mode is dependent only on E_x, H_y and H_x, and that the TM mode is dependent only on H_x, E_y and E_z. Due to the decoupling of modes in 2D, the impedance tensor relation reduces to

$$\begin{bmatrix} E_x \\ E_y \end{bmatrix} = \begin{bmatrix} 0 & Z_{xy} \\ Z_{yx} & 0 \end{bmatrix} \begin{bmatrix} H_x \\ H_y \end{bmatrix} \qquad (4)$$

where $Z_{xy} \neq Z_{yx}$.

The apparent resistivity ρ_a and phase ϕ of the subsurface can be determined by (Telford et al., 1990)

$$\rho_a = \frac{1}{\mu\omega}[Z]^2 \text{ and } \phi = \arctan(Z) \quad (5)$$

where Z is either Z_{xy} for the TE mode or Z_{yx} for the TM mode.

At a boundary between two media of different conductivities σ_1 and σ_2, the following boundary conditions must be obeyed (Swift, 1971):

- The component of B perpendicular to the interface (μH_y) is continuous.
- The component of H parallel to the interface (H_x) is continuous.
- The component of E parallel to the interface (E_x) is continuous.
- The current density J perpendicular to the interface (σE_y) is continuous.

The only discontinuous quantities are J_x and E_y, the current density parallel to and the electric field perpendicular to the interface. Consider an interface (eg a vertical fault) separating uniform quarter-spaces of conductivities σ_1 and σ_2 respectively. The interface strikes in the x direction, and the inducing electric field is in the y direction (TM mode), as illustrated in Figure 1. Several authors (Wannamaker et al., 1984a; Vozoff, 1991; and Jones, 1983) explain that charge distributions build up in the region of the interface. These charge distributions, often referred to as current gathering or boundary charges, produce electric fields in the –y and y directions. These secondary fields add vectorially to the inducing E_y field in each medium. On the more conductive side, the resultant electric field is

$$E_{res} = Ey_{primary} - Ey_{secondary}. \quad (6)$$

This decrease in the electric field reflects a decrease of apparent resistivity. Similarly, on the more resistive side of the fault, the resultant electric field is

$$E_{res} = Ey_{primary} + Ey_{secondary} \quad (7)$$

and the increase in the electric field increases the apparent resistivity (Argawal et al., 1993). Jones (1983) points out that the impact of these secondary electric fields are manifest only for a given equilibrium distance from the interface, defined as being proportional to $l\delta_h^{-1}$, where l is the length of the inhomogeneity and δ_h is the skin depth (in metres) in the host rock of resistivity ρ (in ohm-m), given by (Telford et al., 1996)

$$\delta_h \approx 500(\rho T)^{1/2} m \quad (8)$$

where T is the period in seconds. At distances greater than the equilibrium distance from an interface, correct values of apparent resistivity will be detected. The equilibrium distance for the TM mode is quite small and accurate models can be made even when $\ell << \delta_h$.

Current gathering allows accurate delineation of the boundaries of anomalies in the TM mode, but means that the apparent resistivities of the surrounding regions will not be determined accurately. However, in most TM modelling codes this is taken into account (Wannamaker et al., 1984a) and the apparent resistivities are correctly output. In comparison, the TE mode will not be affected by current gathering, as current flow is parallel to the resistivity interface. As current flows parallel to conductivity interfaces in the TE mode, TE models do not define boundaries as accurately as TM models (Argawal et al., 1993) unless the bodies are small compared to the sin-depth (Jones, 1983)

All naturally occurring geological bodies are of course 3D and there is no simple separation into TE and TM modes. However in practice the assumption is often made that an elongate 3D inhomogeneity can be approximated by a 2D structure closely enough at some scale such that TE and TM decoupling holds. This assumption is made because 3D processing and modelling routines are currently slow and are not easily amenable to inversion (Rodi et al., 1995). Therefore, data for elongate 3D heterogeneities are often collected and interpreted using 2D strategies.

Given this assumption, it is vital that processing, modelling and interpretation do not proceed with a 'black box' mentality in which 2D strategies are applied to the data with no consideration of the errors that this may introduce. We will assess the impact that the 3-dimensionality of an elongate 3D body has on the results of 2D processes that are applied to it. By this, we aim to analyse the applicability of using 2D processes on the 3D body and to note some useful checks that can be made to safeguard from unconstrained errors.

In an elongate 3D body, current gathering is clearly a concern in all orientations since induced electric currents J in all directions encounter boundaries at which there are changes in conductivity (Wannamaker et al., 1984a,b). Current gathering in the assumed TE mode acts in an analogous fashion to current gathering in the TM mode, resulting in a general depression in values of apparent resistivity along the conductor (Wannamaker, 2002, pers. comm.). However, since current gathering is not a feature of 2D TE processes, 2D modelling algorithms do not take current gathering in the TE mode into account so TE models over 3D heterogeneities interpret anomalously low apparent resistivities. Jones (1983) notes that the equilibrium distance for the TE mode is much greater than that in the TM mode and suggests that the profile should be at least one host medium skin depth away from any conductivity interfaces in the direction of strike for current gathering effects to be insignificant. In this study, we will compare TE and TM mode models, as well as comparing models from lines close to the centre of the body with those from lines close to the edge of the body to assess the impact of current gathering and the equilibrium distance in this 3D body.

Regolith poses a further complication in the 2D interpretation of MT data due to galvanic scattering by small-scale near-surface conductivity inhomogeneities (Chave and Smith, 1994; Lilley, 1998a). Even if a basement target body is approximately 2D, galvanic scattering in overlying 3D regolith

may produce 3D results. Many methods have been developed to determine the dimensionality of a region of investigation and to distinguish and then remove any galvanic scattering from the data (eg Bahr, 1988; Groom and Bailey, 1989, 1991), including intuitively simple approaches developed by Lilley (Lilley 1998a,b) which will be utilised here. The potential of galvanic scattering to affect TM data is often not even considered in both commercial and research surveys. In this study we aim to assess the impact of regolith scattering on the 2D assumption at the Deep Well prospect.

1. FIELD SITE

The geological feature of interest is an antiformal dome defined by an elongate magnetic anomaly with a strike length of 2.5 to 3km (see Figure 2). Analysis of geophysical and drillhole data from the prospect has produced the geological interpretation of the anomaly shown in Figures 3 and 4 (Law, S. R., 2002, pers. comm.), using the lithological divisions of Conor (2000). A 3D magnetic model using the method of Li and Oldenburg (1996) indicates that the body plunges at the northeast and southwest extents. The dome trends in a northeasterly direction and is cut by several faults. Drilling results from the area show that the basement is overlain by approximately 80m of regolith (Figure 4).

Since the target feature is an elongate 3D anomaly, it is an ideal site for analysis of MT data in the presence of an approximately 2D anomaly. The setting approximates 2-dimensionality as closely as most real earth environments, but contains heterogeneities that are not 2D. The two interior lines are particularly expected to see the structure of the anomaly as being 2D, but the two lines on the edge of the anomaly may be more influenced by 3D effects. Analysis of this dataset enables determination of whether processing and modelling under the 2D assumption yields valid results, and whether sufficient information for accurate modelling is obtained by collecting only TM mode data.

The lithological units of importance at the Deep Well Prospect are the Ethiudna Subgroup, the Bimba Formation and the Strathearn Group (Conor, 2001). Metasediments within the Bimba Formation contain disseminated sulphides and sometimes lenses of massive sulphide. Significantly, some of the most substantial sulphide occurrences in the subsurface are closely associated with calc-silicates and carbonates. Since the unit interpreted as the Bimba Formation is composed of carbonates and calc-silicates, and drilling results suggest that it contains significant levels of sulphide, it can be expected to produce a significant conductivity anomaly. The Ethiudna Subgroup is lithologically diverse but is characterised by the presence of calc-silicate minerals and local pyrite dominated mineralisation (Conor, 2001). Locally the Ethiudna Subgroup is predominantly albitic with common occurrences of magnetite. Previous drilling at Deep Well and other areas in close proximity confirmed that the Ethiudna Subgroup is the source of the magnetic anomaly (Law, S. R., 2002, pers. comm.). The Strathearn Group is predominantly pelitic (Conor, 2001) and contains non-uniform graphite occurrences that are also a potential source of conductivity anomalies.

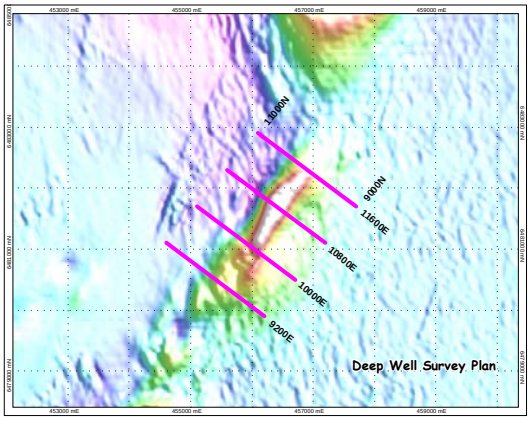

Figure 2. Survey lines are oriented perpendicular to the strike of a magnetic anomaly.

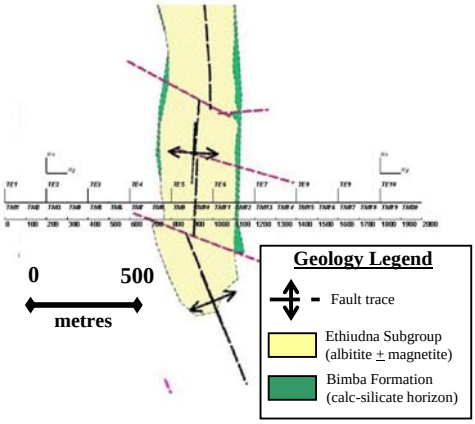

Figure 3. Line layout as illustrated by line 9200E. Each line is 2km long with twenty TM dipoles ten TE dipoles all of length 100m measuring the electric field strength across and along strike of the anomaly. Two sets of magnetometers were used, at 200m and 1800m from the start of the line, each set measured both H_x and H_y. For all processing, the magnetometer at 200m was the primary and the magnetometer at 1800m remote-reference. Also shown is the geological interpretation, plan view. The

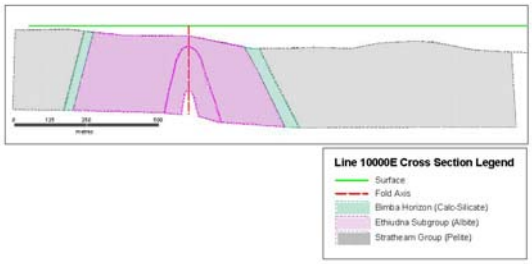

magnetic body is interpreted to be the Ethiudna Subgroup Figure 4. Interpreted geological cross-section of the target body. The target body is an antiformal dome.

1.1 Field Data

Data were collected in February 2002 using the Mount Isa Mines Distributed Acquisition System (MIMDAS) (Sheard, 1998; Garner and Thiel, 2000) at the Deep Well prospect in the Curnamona Province of South Australia. Regionally, this area may be expected to lie within the influence of the "Flinders Conductor", one of the major conductivity anomalous structures of the Australian continent (Wang et al., 1997). The survey consisted of four lines, each 2km long, over an elongated magnetic anomaly target as shown in Figure 2.

The lines are separated by 800m, referenced to a local grid and called 11600E, 10800E, 10000E and 9200E respectively (Figure 2). There is a separation distance of 800m between the lines. Data were collected with an assumption that the underlying structure was 2D. Therefore separate TE and TM dipoles were collected. Taking the strike of the anomaly as the x-direction, the electric field was measured with 100m long dipoles in both the x-direction for the TE mode and the y-direction for the TM mode using electrodes consisting of clay pots filled with copper sulphate solution. Twenty 100m TM dipoles were deployed in a line and ten 100m TE dipoles were laid out every 200m, as shown in Figure 3. Orthogonal component horizontal magnetic fields were measured with EMI BF4 coils buried under approximately 50cm of earth to prevent disturbance by wind and animals. Two sets of magnetic measurements were taken on each line, such that H_x and H_y measurements were taken at sites 200m and 1800m along the lines to allow for remote reference processing (Gamble et al., 1979; Chave and Thomson, 1989). For all processing, the magnetometer at 200m was the primary and the magnetometer at 1800m the remote-reference.

Data were sampled at 1600Hz for a total sampling interval of 154.88s. This sampling process was repeated a number of times for each line; each repetition is referred to as an 'event'. Of these, between eleven and eighteen events for each line produced data with sufficiently high signal to noise ratio for each line to be useful.

2. DATA PROCESSING

2.1 Comparison of Methods

Data from this survey were processed using three algorithms as a comparison: a single-station, robust, remote-reference method (RRRMT; Chave et al., 1987; Chave and Thomson, 1989), a multi-station array, robust, remote-referenced method (Egbert, 1997) and an in-house code developed by MIM (Terry Ritchie, 2002, pers. comm.) The three main points of comparison between these methods are the use of robust statistics, remote referencing and multivariate statistics.

RRRMT and Egbert's code both use robust statistics to remove non-Gaussian data outliers, which are a hindrance to the determination of MT impedances and errors. Robust techniques are efficient because they are insensitive to a moderate amount of contaminated data or to inadequacies in the model and react gradually rather than abruptly to disturbances in either the data or the model (Chave et al., 1987). RRRMT and MIM's code both use a remote reference to reduce incoherent noise (Gamble et al., 1979; Chave and Thomson, 1989). Remote magnetic field measurements are taken at a reference point some distance away from the site of primary magnetic field measurement. Differences between the remote and primary magnetic field measurements are taken to be incoherent noise and are downweighted or removed from the data with a dramatic improvement in data quality. Egbert's code (Egbert, 1997) utilises multivariate statistics in contrast to the univariate statistics of RRRMT and MIM. Univariate statistics consider each channel separately whereas multivariate statistics consider all of the collected channels together. This has two significant advantages over univariate statistics. Firstly, this approach includes the remote reference principle but extends it by using every available magnetic channel to remove the maximum amount of incoherent noise. Secondly it estimates the amplitude of incoherent noise in each channel and then removes this incoherent noise. This allows the number of sources of coherent signal to be determined to test for the presence of coherent noise.

The phase results are very similar for each processing technique in the period-range where the data have small errors, although at periods less than approximately $3\times10^{-3}s$ the results from Egbert's code follow the trend of the data more smoothly. The different processing techniques also gave very comparable results for apparent resistivity. It is reasonable to expect that the advantages that Egbert's code offers over RRRMT and MIM processing would not be very valuable in this situation for two reasons. Firstly, the field area is so remote that coherent noise should be insignificant and secondly each line contains only two pairs of magnetometers, so the multivariate statistics do not remove any more noise in the magnetic field than RRRMT's and MIM's remote referencing. It follows that the best approach in choosing a processing code to use is to treat each situation individually. If several data channels have been read at numerous stations and coherent noise is thought to be a problem, Egbert's code should be used. However if it is known not to be a problem a simpler code such as RRRMT or MIM's in-house code is sufficient.

2.2 Processing Results

Data quality was assessed using coherence plots, which analyse the behaviour of the electric field as the magnetic field changes with time (Chave et al., 1987). Coherence drops off rapidly at a period of 1s, in the dead band. Some sites had low coherence across the whole period range due to low signal strength and could then be excluded from further modelling. Some events were seen to be more noisy than others and the event with the least noise was chosen for further modelling for each line.

Apparent resistivities and phases were determined for the TE and TM modes at each site. All processing methods produce a split in the apparent resistivity values between the TE and TM modes that increases in magnitude with period. In all cases, TM is greater than TE (Figure 5). This split is a clear indication that the region is not ideally 2D. As expected with the loss of signal and low coherence, apparent resistivity values have very large errors at periods greater than 0.1s. At the majority of sites, most of the phase values are greater than 45°, for all periods in the TM mode and for periods greater than 0.1s in the TE mode.

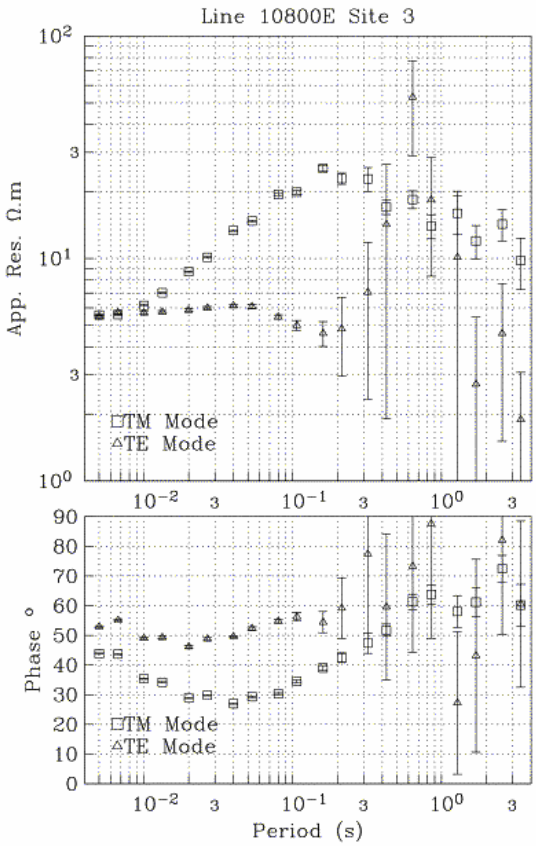

Figure 5. MT responses shown as TE (triangles) and TM (squares) apparent resistivity and phase from a typical site on line 10800E. At periods between 0.1 – 10 s, the coherence is very low in the dead-band and hence the error bars are large.

3. GEOLOGICAL DIMENSIONALITY AND GALVANIC SCATTERING

Analysis was carried out to determine the extent of deviation from 2-dimensionality using both Mohr circles to determine the dimensionality of each site and strike determination to highlight any deviation from a uniform, 2D strike. Galvanic scattering from the regolith will alter the dimensionality of a site, making an underlying 2D basement response 3D and also changing the strike of the signal. Therefore both dimensionality and galvanic effects were analysed with these methods.

3.1 Mohr Circles

Mohr circles (Lilley 1976; Lilley 1993a,b; Lilley 1998a,b) are diagrammatical presentations of MT impedance tensors that clearly demonstrate the dimensionality of the target body. Z'_{xx} is plotted against Z'_{xy}, where these are the values of Z_{xx} and Z_{xy} which would be obtained if the measuring axes were rotated through angle θ' from their original orientation, as shown in Figure 6. The plot describes a circle as the measuring axes rotate through all values of Z'_{xx} and Z'_{xy}. A 1D geological structure is denoted by a point on the horizontal axis, since Z_{xx} =0 and Z_{xy} =-Z_{yx} (Figure 6a). A Mohr circle of data from a 2D structure will be centred on the horizontal axis

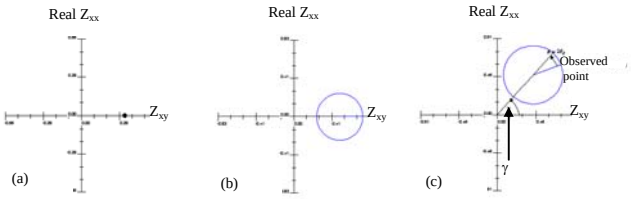

Figure 6. The Mohr circle of (a) 1D earth is a point on the Zxy axis; (b) a 2D earth is a circle with its centre on the Zxy axis; and (c) a 3D earth is a circle offset from the Zxy axis by a skew angle γ.

(Figure 6b) and Mohr circles from a 3D geological structure (either at depth or galvanic scattering in the overlying 3D regolith) will be rotated or 'skewed' above or below the horizontal axis (Figure 6c). The extent of three-dimensionality is measured by the skew angle γ (Figure 6c) between the horizontal axis and a line from the origin passing through the centres of the circles (Lilley 1998a).

Mohr circles from all sites indicate 2D structure with some sites displaying slight 3D characteristics. Sites on the two exterior lines (11600E, 9200E) show weak 3D characteristics compared to those on the interior lines (10000E, 10800E), as would be expected, but these are small at all sites. Figure 7a shows the full frequency range of Mohr circles from the eleventh TM measuring site along line 9200E, which is one of the more pronounced 3D sites and Figure 7b shows the strongly 2D Mohr circle from the seventeenth TM measuring site along line 10000E. It can be seen that the centres of the circles along the entire frequency range track along the horizontal axis, showing the sources to be very strongly 2D.

The strong two-dimensionality of the Mohr circles also demonstrates that galvanic scattering through the regolith is not strongly affecting these data. The regolith may simply be 1D in this area, resulting in no scattering effects. Alternatively, the regolith may be so highly conductive in comparison to the basement that the scattering of the induced currents becomes insignificant.

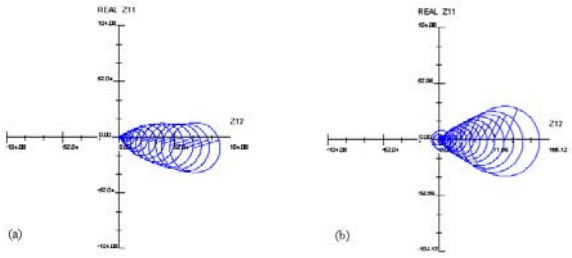

Figure 7. (a) Mohr circles of eleventh TM observing site on line 9200E is one of the most strongly 3D of the survey. Three-dimensionality of this site is seen by the offset of the circle centres from the horizontal axis. (b) Mohr circles from the seventeenth TM observing site on line 10000E. Strong two-dimensionality is seen by the fact that the centres of all of the circles sit on the horizontal axis.

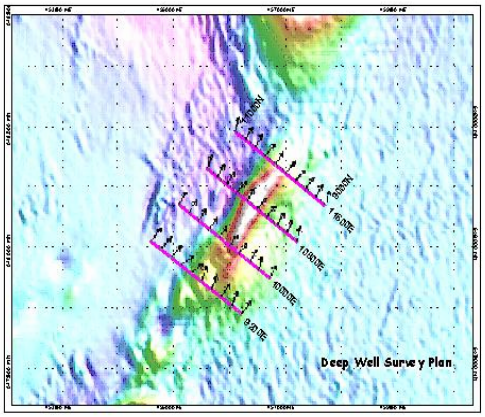

Figure 8. Direction of the electric field strike over period range 10^{-2} to 10^{-1}s determined using Lilley's (1998a) method. The electric field strike approximates the strike of the local geology. Pink lines and vertical ticks show direction of observing axes.

3.2 Local and Regional Strike

Profile lines were oriented orthogonal to the strike of the magnetic anomaly. Deviation of the electrical strike from the magnetic strike was determined using Lilley angles (Lilley 1995). Both twist operators and split operators can act upon 1D impedance tensors to give 3D impedance tensors. The twist tensor **T** has the effect of rotating either the electric or magnetic field clockwise through angle ψ, and is defined as

$$\mathbf{T} = \begin{bmatrix} \cos\psi & \sin\psi \\ -\sin\psi & \cos\psi \end{bmatrix} \tag{9}$$

The split tensor **S** is analogous to the pure shear operator (Means 1990). It does not involve any rotational components but instead stretches the tensor data and is defined as

$$\mathbf{S} = \begin{bmatrix} 1+S & 0 \\ 0 & 1-S \end{bmatrix} \tag{10}$$

where S is the extent of splitting or stretch on the data.

Such operators can act on a 1D impedance tensor in two ways; twist before split, defined as 'Path 1' and split before twist, defined as 'Path 2'. These two paths give different values for θ', the angle of rotation of the observing axes clockwise from their alignment with the splitting axes. For Path 1,

$$\mathbf{Z}_{obs} = g\mathbf{TSZ}_{basement} \tag{11}$$

$$\theta' = -\theta_e \tag{12}$$

where θ_e is the electric field direction anticlockwise from the measuring axes and g is the static shift parameter. For Path 2,

$$\mathbf{Z}_{obs} = g\mathbf{STZ}_{basement} \tag{13}$$

$$\theta' = -\theta_h \tag{14}$$

where θ_h is the magnetic field direction anticlockwise from the measuring axes (Lilley 1995).

Since the magnetic field is affected by the integrated electric field over a region while the electric field is more locally affected, the magnetic field direction, θ_h, is taken to be the strike of the regional geology and the electric field direction, θ_e, is taken to be the strike of the local geology. Therefore, electric field strike was analysed to further determine the shape of the target and identify any galvanic scattering.

The magnetic field strike was aligned with the measuring axes and as shown in Figure 8, the electric field direction deviated only slightly from this, with a mean deviation of ~2°, and a standard deviation of ~10°. It appears therefore that the basement response is not distorted by regolith scattering. Strike direction deviates more on line 9200E than the other lines, supporting the interpretation of the geology, magnetics and Mohr circles that the target body is more 3D here. The strike direction on line 11600E is quite uniform, suggesting that the folded structure continues with constant strike at depth.

4. 2D INVERSION OF 3D STRUCTURES

4.1 Modelling

Data were modelled using inversion codes of Occam (de-Groot Hedlin and Constable, 1990) and non-linear conjugate gradients (NLCG) (Rodi and Mackie, 2001). Inversions were run using TM only, TE only and joint TE-TM data for all lines using both inversion codes. Starting models were uniform half-spaces of 100 ohm.m resistivity. Floor errors were initially set to 1% for both apparent resistivity and phase for TE, TM and joint inversions, such that if any data point had an error smaller than 1% of the data value this error was increased to 1% to improve data fit. The floor errors for joint NLCG inversion were later revised to 5% to enable the inversions to reach the target RMS.

Occam's inversion is based on Newton's method (Constable et al., 1987), in which an objective function is minimised over the space of models to produce an optimal solution of the non-linear inverse problem. The model is overparameterised into more blocks than there are degrees of freedom allowed from the data. The algorithm then solves specifically to minimise model roughness, following the approach of Occam's Razor: that a simple solution is preferable to one which is unnecessarily complicated.

Noting that the computational burden of the Jacobean is an impediment to the development and usefulness of 2D and 3D inversions, Rodi and Mackie (2001) employ the method of (NLCG) described in Polak (1971) and Luenberger (1984). Madden and Mackie (1993) show that operations with the Jacobean and its transpose can be achieved without having to actually compute the Jacobean using the method of conjugate gradients. The NLCG algorithm proceeds from this premise and abandons completely the structure of iterated and linearised inversions. Instead, NLCG performs a sequence of line searches along computed search directions to solve the minimisation problem.

Both algorithms generally reproduced the main features imaged in the corresponding models. In general, Occam models converged to a lower rms value in fewer iterations than NLCG, and the resulting models were generally smoother. Therefore the models shown in Figure 9 and Figure 10 are the Occam models.

4.2 Comparison of Models

All of the models imaged a highly conductive layer extending from the surface to a depth of approximately 80m, interpreted to be the regolith. While the sampling frequencies were not high enough (> 10^3 Hz) to resolve significant structure within the regolith, the apparent resistivity of the region is approximately 4 Ω.m. Results and interpretation of the interior pair of lines 10800E and 10000E are very similar, as are the exterior lines 9200E and 11600E. Therefore only lines 10800E and 11600E will be discussed as they illustrate the conclusions sufficiently.

4.3 Interior Line (10800E)

The TM model of line 10800E images two zones with resistivities less than 10 Ω.m towards the centre of the profiles, labelled BE and BW respectively on Figure 9a. The western body, BW, dips toward the west and extends from a depth of 100 m. The eastern body, BE, has a similar depth extent but dips to the east. These bodies are interpreted as being folded layers of the sulphide rich Bimba Formation. Between the lenses of the Bimba Formation is a resistive block with an apparent resistivity approximately of 100 Ω.m, interpreted to be the Ethiudna Subgroup and labelled E on Figure 9a. This interpreted position of the Ethiudna Subgroup correlates well to its position interpreted from magnetic data (Figure 9a). Two additional conductive regions at approximately 200m and 1800m along the lines are labelled SE and SW and are interpreted as being folded graphitic sections of the Strathearn Group. These have similar depth extents to the Bimba Formation bodies and appear to dip slightly towards the centres of the lines. Remaining areas above approximately 600m have resistivity values >100 Ω.m and are interpreted to be non-graphite bearing Strathearn Group. There is a very good correlation between the modelled positions of these bodies and their expected positions from the geological interpretation. Below 600m the model imaged uniform low resistivity, but the resolving power is minimal at this depth.

In contrast, the TE model has resolved very little structure (Figure 9b). Two regions of low resistivity correspond to locations of Bimba Formation and graphitic Strathearn Group on the western and eastern sides of the line (BSW and BSE). However, the model does not distinguish between the Bimba Formation and the Strathearn Group in these low resistivity regions. Resistivities are generally depressed in the TE mode and values do not exceed ~30 Ω.m. Joint inversions for both lines (Figure 9c) are very similar to the TM inversions.

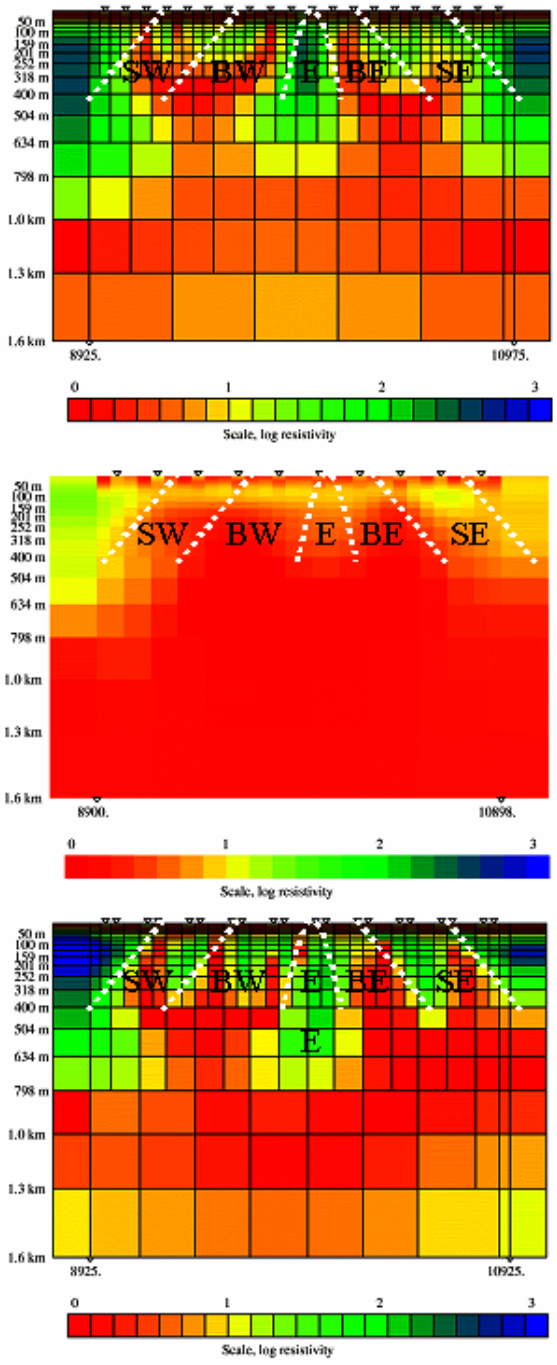

Figure 9. Occam models of line 10800E. (a) TM model, with western Bimba Formation (BW), eastern Bimba Formation (BE), western graphitic Strathearn Group (SW), eastern graphitic Strathearn Group (SE) and Ethiudna Subgroup (E) shown. (b) TE model which poorly resolves a diffuse conductor at the location of BW and SW (BSW) and another diffuse conductor at the location of BE and SE (BSE). (c) Joint TE and TM model which shows many of the same features as (a).

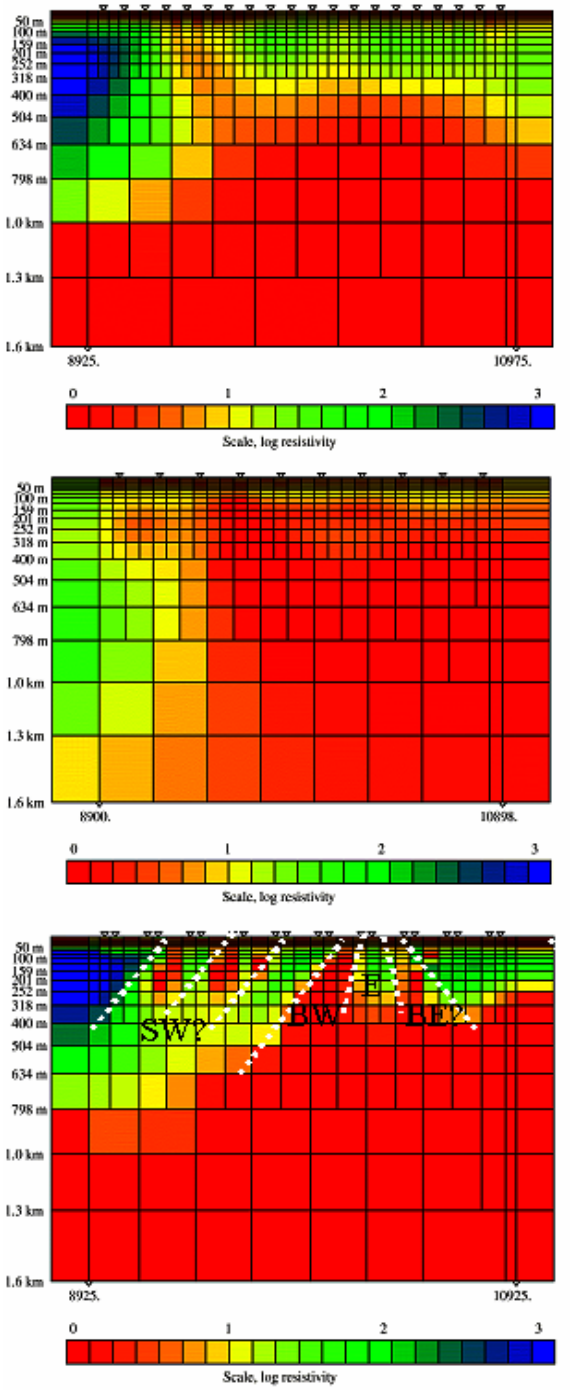

Figure 10. Occam models of line 11600E. (a) TM model. (b) TE model. (c) Joint TE and TM model with interpreted Bimba Formation (BW), eastern Bimba Formation (BE), western graphitic Strathearn Group (SW) and Ethiudna Subgroup (E) shown

4.4 Exterior Line (11600E)

The TM model of line 11600E (Figure 10a) shows significantly less structure than the TM model of line 10800E. A large, diffuse conductor of resistivity less than 1 Ω.m., extending from a depth of 300 m is evident. Above this, a few poorly resolved conductors extend toward the surface in the same locations as the Bimba Formation and graphitic Strathearn Group conductors in line 10800E. The rest of the region has an apparent resistivity ranging between 100 and 1000 Ω.m.

The TE model (Figure 10b) shows even less structure, imaging a highly conductive structure with resistivity < 0.5 Ω.m extending east from 500m along the line and abutting a more resistive structure of resistivity ~30 Ω.m to the west. Of particular note are the very low resistivities in the TE mode. Joint inversions for both lines define more structure than can be related to interpreted subsurface geology (Figure 10c).

DISCUSSION

The extent of deviation from ideal 2-dimensionality of the elongate 3D target body was determined using Mohr circles, which proved an intuitively simple approach. At the skin depth of investigation, the body was remarkably 2D, particularly at it centre, with more pronounced 3D effects at its northeast and southwest extents.

Galvanic scattering due to 3D regolith did not affect these data. This is a surprising result given that there is a significant depth of regolith, which cannot be expected to have the same structural characteristics as the basement, overlying the target body. It may be that the regolith is 1D in this area with the result that it does not scatter the 2D basement response. Alternatively, the regolith may be so highly conductive relative to the basement that the scattering of the induced currents is insignificant. Whatever the cause, it is certainly an advantage that these data are not affected by galvanic scattering as this can be difficult to remove from the desired tensor. Regolith poses a significant challenge throughout Australia as it can obscure the geophysical response from basement bodies of interest. Further work should be done to test whether it can be generalised that the regolith does not galvanically scatter basement MT responses.

Current gathering has had a significant effect on the MT data in three ways. Firstly, boundary definition is much better in the TM mode than the TE mode. The bodies expected to be imaged from the geological interpretation (named BE, BW, SE and SW) are clearly defined in the TM inversions of lines 10000E and 10800E since current gathering occurs at the resistivity interfaces of these bodies. However current gathering does not occur at these boundaries in the TE mode and the bodies are consequently much less well defined in the corresponding TE models. Secondly, current gathering has caused a significant depression of the values of apparent resistivity in the TE mode. TM models all have higher and more realistic resistivity values than do the TE models. Thirdly, the lines closest to the edge of the anomaly (9200E and 11600E) have poorer boundary definition and more unrealistic apparent resistivity values than the interior lines. This is in keeping with the equilibrium distance theory of Jones (1983), which suggests that TE measurements need to be taken a distance of at least one skin-depth (in the host medium) away from resistivity interfaces perpendicular to the inducing field for current gathering effects to become negligible. The skin-depth is variable with respect to the signal-period, but by this definition the TE mode in the central lines will be affected

by current gathering at periods greater than 0.1s and the outer lines will be affected at all measured periods.

Ideally, MT data from all 3D bodies should be processed and modelled with 3D algorithms. However, the current state of play of computing often renders this impractical. It is therefore vital that care is taken to prevent unnecessary errors in analysis and interpretation from a lack of consideration of the 2D assumption that has been made. We recommend that the dimensionality and strike of the region be determined to understand the structure of the inhomogeneity. This allows further analysis to be conducted where the body is most 2D and the establishment of whether galvanic scattering is affecting the observations. The equilibrium distance for the period range of investigation should also be determined so that the unrealistically low TE mode apparent resistivity values in the affected regions can be accounted for. We have found TM mode models to be considerably more useful for interpretation due to their superior boundary definition and realistic apparent resistivity values, but it is still important to collect TE mode data so that appropriate analysis of the region can be made.

ACKNOWLEDGMENTS

The authors thank MIM Exploration and particularly Mr Terry Ritchie and Mr Steven Law for their backing in providing field data, software, hardware, logistical support and much experience. Dr Phil Wannamaker is gratefully acknowledged for helpful correspondence, as are Dr Nick Direen and Prof. Stewart Greenhalgh for their valuable comments and suggestions. We are grateful to Louise Pellerin and an anonymous reviewer for their very valuable reviews. This study was funded by the CRC LEME and an ASEG Research Foundation Grant.

REFERENCES

Agarwal, A. K., Poll, H. E. and Weaver, J. T., 1993, One- and two-dimensional inversion of magnetotelluric data in continental regions: Physics of the Earth and Planetary Interiors, 81, 155-176.

Bahr, K., 1988, Interpretation of the magnetotelluric impedance tensor: Regional induction and local telluric distortion: Journal of Geophysics 62, 119-127.

Chave, A. D., Thomson, D. J. and Ander, M. E., 1987, On the robust estimation of power spectra, coherences, and transfer functions: Journal of Geophysical Research, 92, 633-648.

Chave, A. D., and Thomson, D. J., 1989, Some comments on magnetotelluric response function estimation: Journal of Geophysical Research 94, 14215-14225.

Chave, A. D., and Smith, J. T., 1994, On electric and magnetic galvanic distortion tensor decomposition: Journal of Geophysical Research 99, 4669-4682.

Conor, C. H. H., 2000, Definition of major sedimentary and igneous units of the Olary Domain, Curnamona Province: MESA Journal 19, 51-56.

Conor, C. H., 2001, Geology of the Olary Domain, Curnamona Province, South Australia: Primary Industries and Resources South Australia, 1-15.

Constable, S. C., Parker, R. L. and Constable, C. G., 1987, Occam's inversion: a practical algorithm for generating smooth models from EM sounding data: Geophysics 52, 289-300.

deGroot-Hedlin, C. and Constable, S., 1990, Occam's inversion to generate smooth, two-dimensional models from magnetotelluric data: Geophysics 55, 1613-1624.

Egbert, G. E., 1997, Robust multiple-station magnetotelluric data processing: Geophysical Journal International 130, 475-496.

Gamble, T. D., Goubau, W. M. and Clarke, J., 1979, Magnetotellurics with a remote reference: Geophysics 44, 53-68.

Garner, S. J. and Thiel, D. V., 2000, Broadband (ULF-VLF) surface impedance measurements using MIMDAS: Exploration Geophysics 31, 173-178.

Groom, R. W., and Bailey, R. C., 1989, Decomposition of magnetotelluric impedance tensors in the presence of local three-dimensional galvanic distortion: Journal of Geophysical Research 94, 1913-1925.

Groom, R. W., and Bailey, R. C., 1991, Analytic investigations of the effects of near-surface three-dimensional galvanic scatterers on MT tensor decompositions: Geophysics 51, 496-518.

Jones, A. G., 1983, The problem of current channelling: A critical review: Geophysical Surveys 6, 79-122.

Li, Y and Oldenburg, D. W., 1996, 3D inversion of magnetic data: Geophysics 61, 394-408.

Lilley, F. E. M., 1976, Short Note: Diagrams for magnetotelluric data: Geophysics 41, 766-770.

Lilley, F. E. M., 1993a, Magnetotelluric analysis using Mohr circles: Geophysics 58, 1498-1506.

Lilley, F. E. M., 1993b, Three-dimensionality of the BC87 magnetotelluric data set studied using Mohr circles: J. Geomag. Geoelectr. 45, 1107-1113.

Lilley, F. E. M., 1995, Strike direction: obtained from basic models for 3D magnetotelluric data, in: Oristaglio, M. and Spies, B., eds, Three-Dimensional Electromagnetics, Schlumberger-Doll Research, 359-369.

Lilley, F. E. M., 1998a, Magnetotelluric tensor decomposition: Part 1, Theory for a basic procedure: Geophysics 63, 1885-1897.

Lilley, F. E. M., 1998b, Magnetotelluric tensor decomposition: Part 2, Examples of a basic procedure: Geophysics 63, 1898-1907.

Luenberger, D. G., 1984, Linear and nonlinear programming, 2nd Ed.: Addison-Wesley Publ. Co.

Madden, T. R. and Mackie, R. L., 1993, Three-dimensional magnetotelluric inversion using conjugate gradients: Geophysical Journal International, 115, 215-229.

Means, W. D., 1990, Review paper: Kinematics, stress, deformation and material behaviour: Journal of Structural Geology 12, 953-971.

Patra, H. P. and Mallick, K., 1980, Geosounding Principles, 2 time-varying geoelectric soundings: Elsevier, pp 449 .

Polak, E., 1971, Computational methods in optimisation: A unified approach: Academic Press.

Rodi, W. and Mackie, R. L., 2001, Nonlinear conjugate gradients algorithm for 2-D magnetotelluric inversion: Geophysics 66, 174-187.

Sheard, S. N., 1998, MIMDAS - a new direction in geophysics, 13th bi-annual conference, Australian Society of Exploration Geophysics: Abstracts, Preview 76, 104.

Swift, C. M. Jr., 1971, Theoretical magnetotelluric and turam response from two-dimensional inhomogeneities: Geophysics 36, 38-52.

Telford, W. M., Geldart, L. P., and Sheriff, R. E., 1990, Applied Geophysics, Second Edition: Cambridge University Press.

Vozoff, K., 1991, The magnetotelluric method, in Nabighian, M. N., (ed.), Electromagnetic methods in applied geophysics – Applications Part A and Part B: Society of Exploration Geophysicists, 641-713.

Wang, L.J., Lilley, F.E.M. and Chamalaun, F.H., 1997, Large-scale electrical conductivity structure of Australia from magnetometer arrays: Exploration Geophysics 28, 150-155.

Wannamaker, P. E., Hohmann, G. W. and Ward, S. H., 1984a, Magnetotelluric responses of three-dimensional bodies in layered earths: Geophysics 49, 1517-1533.

Wannamaker, P. E., Hohmann, G. W., and San Filipo, W. A., 1984b, Electromagnetic modelling of three-dimensional bodies in layered earths using integral equations: Geophysics 49, 60-74.